



Contents lists available at SciVerse ScienceDirect

Nonlinear Analysis: Real World Applications

journal homepage: www.elsevier.com/locate/nonrwa

Global dynamics of a mathematical model for HTLV-I infection of CD4⁺ T cells with delayed CTL response

Michael Y. Li, Hongying Shu*

Department of Mathematics, Harbin Institute of Technology, Harbin, Heilongjiang 150001, PR China

Department of Mathematical and Statistical Sciences, University of Alberta, Edmonton, Alberta, T6G 2G1, Canada

ARTICLE INFO

Article history:

Received 4 May 2010

Accepted 18 February 2011

Keywords:

In-host models

HTLV-I infection

HAM/TSP

CTL response

Time delays

Lyapunov functional

Hopf bifurcation

ABSTRACT

Human T-cell leukaemia virus type I (HTLV-I) preferentially infects the CD4⁺ T cells. The HTLV-I infection causes a strong HTLV-I specific immune response from CD8⁺ cytotoxic T cells (CTLs). The persistent cytotoxicity of the CTL is believed to contribute to the development of a progressive neurologic disease, HTLV-I associated myelopathy/tropical spastic paraparesis (HAM/TSP). We investigate the global dynamics of a mathematical model for the CTL response to HTLV-I infection *in vivo*. To account for a series of immunological events leading to the CTL response, we incorporate a time delay in the response term. Our mathematical analysis establishes that the global dynamics are determined by two threshold parameters R_0 and R_1 , basic reproduction numbers for viral infection and for CTL response, respectively. If $R_0 \leq 1$, the infection-free equilibrium P_0 is globally asymptotically stable, and the HTLV-I viruses are cleared. If $R_1 \leq 1 < R_0$, the asymptomatic-carrier equilibrium P_1 is globally asymptotically stable, and the HTLV-I infection becomes chronic but with no persistent CTL response. If $R_1 > 1$, a unique HAM/TSP equilibrium P_2 exists, at which the HTLV-I infection is chronic with a persistent CTL response. We show that the time delay can destabilize the HAM/TSP equilibrium, leading to Hopf bifurcations and stable periodic oscillations. Implications of our results to the pathogenesis of HTLV-I infection and HAM/TSP development are discussed.

© 2011 Elsevier Ltd. All rights reserved.

1. Introduction

Recently, the study of population dynamics of infectious diseases has attracted much attention. Several mathematical models have been proposed to describe the *in vivo* infection process with humoral immune response such as human immunodeficiency virus (HIV), hepatitis B virus (HBV), and human T-cell leukemia virus type I (HTLV-I) [1–5]. These in-host models can capture some essential features of the immune system and are able to produce a variety of immune responses many of which are observed experimentally and clinically. Findings from in-host modeling can also be used to guide the development of efficient antiviral drug therapies.

Because of the importance of the biological meanings, dynamical properties of HTLV-I infection models have been studied by many authors [6–10]. HTLV-I is the etiologic agent in a progressive human neurologic disease, the HTLV-I associated myelopathy/tropical spastic paraparesis (HAM/TSP) [11,12]. HTLV-I infection is also known to cause adult T-cell leukemia (ATL) among other human diseases [13,14]. Approximately 20 to 40 million people are infected by HTLV-I worldwide, mostly in the Caribbean, southern Japan, Central and South America, the Middle East, and equatorial Africa [15]. The majority of HTLV-I infected individuals remain lifelong asymptomatic carriers. Approximately 0.25%–3.8% of infected individuals develop HAM/TSP, and another 2%–3% develop ATL [6]. HTLV-I preferentially infects CD4⁺ helper T cells [6]. HTLV-I infection

* Corresponding author at: Department of Mathematics, Harbin Institute of Technology, Harbin, Heilongjiang 150001, PR China.

E-mail addresses: shuhongying08@gmail.com, hyshu@math.ualberta.ca (H. Shu).

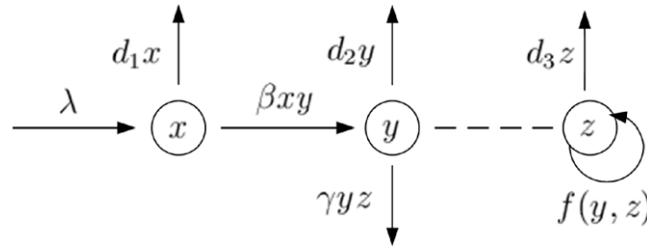


Fig. 1. Transfer diagram of HTLV-I infection with CTL response.

in vivo is achieved through cell-to-cell contact among healthy and infected CD4⁺ T cells [7]. The immune system reacts to HTLV-I infection with a strong cytotoxic T-lymphocyte (CTL) response [6,8]. On one hand, CTL has a protective role by regulating the proviral load, and on the other hand, evidence suggests that cytotoxicity of the CTL is ultimately responsible for the demyelination of the central nervous system resulting in HAM/TSP [6,8]. Understanding the role played by the CTL response in controlling the HTLV-I infection is essential for identifying risk factors for the development of HAM/TSP and for designing therapeutic measures. Mathematical models have been developed to describe the interaction *in vivo* among HTLV-I, the CD4⁺ target cells, and the CTL immune response [16–18,9,10], and used as a tool to study the role of immune response in the viral dynamics.

To set up a HTLV-I infection model with CTL response, we partition the CD4⁺ T-cell population into uninfected and infected compartments, whose numbers at time t are denoted by $x(t)$, $y(t)$, respectively. Let $z(t)$ denote the number of HTLV-I-specific CD8⁺ CTLs at time t . The production of healthy CD4⁺ T cells is assumed to be at a constant rate λ [19]. Since HTLV-I infection occurs by cell-to-cell contact between infected cells and uninfected cells, a bilinear incidence βxy is assumed [19,17]. CTL-driven elimination of infected CD4⁺ cells is assumed to be of the form γyz , where γ is the rate of CTL elimination. The CTL response to HTLV-I infection is modeled by a general function $f(y, z)$, dependent of the number of CTLs and infected CD4⁺ T cells. The turnover rates of uninfected and infected CD4⁺ T cells are d_1 and d_2 , respectively, and the turnover rate of CTLs is d_3 . All parameters are assumed to be positive. A transfer diagram for the transmission of CTL response to HTLV-I infection is shown in Fig. 1.

The preceding assumptions and the transfer diagram lead to the following basic HTLV-I infection model with CTL response

$$\begin{aligned} x'(t) &= \lambda - d_1x(t) - \beta x(t)y(t), \\ y'(t) &= \beta x(t)y(t) - d_2y(t) - \gamma y(t)z(t), \\ z'(t) &= f(y, z) - d_3z(t). \end{aligned} \tag{1}$$

This model with several forms of CTL response function $f(y, z)$ have been considered and analyzed in the literature [16,20–22].

Antigenic stimulation that generates HTLV-I specific CTLs involves a sequence of events and requires a time lag [23,24]. As a consequence, the CTLs produced at time t may depend on the number of CTLs and infected target cells at time $t - \tau$, for a time lag $\tau > 0$. Accordingly, the CTL response in (1) can be more realistically modeled by $f(y(t - \tau), z(t - \tau))$, and model (1) replaced by a system of delayed differential equations. Recent studies of HTLV-I infection models with delayed CTL response were carried out in [23,24]. It is shown through numerical simulations that delayed CTL response can lead to sustained oscillations.

In the present paper, we assume $f(y, z) = \mu yz$ and incorporate a time delay into the immune response in (1) to obtain the following model

$$\begin{aligned} x'(t) &= \lambda - d_1x(t) - \beta x(t)y(t), \\ y'(t) &= \beta x(t)y(t) - d_2y(t) - \gamma y(t)z(t), \\ z'(t) &= \mu y(t - \tau)z(t - \tau) - d_3z(t). \end{aligned} \tag{2}$$

Model (2) was considered in Wang et al. [24] and its dynamics explored numerically. Our goal in this paper is to carry out rigorous mathematical analysis of dynamic behaviors of system (2). We will show that the global dynamics of model (2) are determined by two key threshold parameters R_0 and R_1 as given in (4) and (5), which are termed as the basic reproduction numbers for viral infection and for CTL response, respectively (cf. [10]). More specifically, if $R_0 \leq 1$, the infection-free equilibrium P_0 is globally asymptotically stable, and the HTLV-I viruses are cleared. If $R_1 \leq 1 < R_0$, there exists a carrier equilibrium P_1 and it is globally asymptotically stable. In this case, the HTLV-I infection becomes chronic but there is no established CTL response an risk of HAM/TSP development. If $R_1 > 1$, there exists a HAM/TSP equilibrium P_2 , at which the HTLV-I infection is chronic and the CTL response is persistent, as is the risk for HAM/TSP. We show that the time delay can destabilize P_2 and lead to Hopf bifurcations. Using normal form and center manifold theory, we determine the stability of bifurcating periodic solutions.

Periodic oscillations have been shown to exist in in-host models for HTLV-I infection and CTL response. Wodarz et al. [16] have shown that periodic oscillations can occur with CTL response and mitosis in infected CD4⁺ T cells. Wang et al. [24]

have shown that time delays can induce Hopf bifurcations in a model that is similar to system (2). These earlier works in the literature rely mainly on numerical simulations. Our results are the first to establish the existence of Hopf bifurcation in a HTLV-I model with immune response and time delays using rigorous mathematical analysis. Compared to numerical results in earlier studies such as Wang et al. [24], our mathematical analysis reveals the existence of the carrier equilibrium P_1 and a separate threshold parameter R_1 , which are neglected in [16,24]. The fact that P_1 can be globally stable for a large range of parameter values justifies the need for rigorous analysis. Since P_1 can represent the state of asymptotic carriers of HTLV-I, its stability analysis and the associated threshold parameter R_1 have significant implications for the control of HTLV-I associated diseases such as HAM/TSP. Our results are also related to earlier studies on the impact of delays on models of viral infections without immune response. In Li and Shu [25], it is shown that whether intracellular delays can cause periodic oscillations is critically connected to the target cell dynamics: if the target cell dynamics do not contain a mitosis component, then intracellular delays in the viral infection will not cause sustained oscillations. Our results in the present paper show that a mitosis component is not required for sustained oscillations to occur when the immune response is incorporated in to the model. These results together have enriched our understanding of the effects of intracellular delays in viral infection processes and its interaction with the immune response.

The paper is organized as follows. In the next section, the threshold parameters R_0 and R_1 are derived and existence of equilibria are discussed in relation to values of R_0 and R_1 . In Sections 3 and 4, global stability of P_0 and P_1 are established using global Lyapunov functionals that are motivated by the work in [26]. In Section 5, we consider stability of the HAM/TSP equilibrium P_2 and the occurrence of local Hopf bifurcation using the delay τ as a bifurcation parameter. Stability of the bifurcating periodic solutions is also analyzed in this section. Results from numerical simulations are presented in Section 6, to illustrate and support our analytical results. Biological implications of our results are discussed in Section 7.

2. Preliminaries

To investigate the dynamics of system (2), we need to consider a suitable phase space and a feasible region. For $\tau > 0$, we denote by $\mathcal{C} = \mathcal{C}([-\tau, 0], \mathbb{R})$ the Banach space of continuous real-valued functions on the interval $[-\tau, 0]$, with norm $\|\phi\| = \sup_{-\tau \leq \theta \leq 0} |\phi(\theta)|$ for $\phi \in \mathcal{C}$. The nonnegative cone of \mathcal{C} is defined as $\mathcal{C}^+ = \mathcal{C}([-\tau, 0], \mathbb{R}_+)$. Initial conditions for system (2) are chosen at $t = 0$ as

$$\varphi \in \mathbb{R}_+ \times \mathcal{C}^+ \times \mathcal{C}^+, \quad \varphi(0) > 0. \tag{3}$$

Proposition 2.1. *Under initial conditions in (3), all solutions of system (2) are positive and ultimately bounded in $\mathbb{R} \times \mathcal{C} \times \mathcal{C}$.*

Proof. First, we prove that $x(t)$ is positive for $t \geq 0$. Assuming the contrary and letting $t_1 > 0$ be the first time such that $x(t_1) = 0$, by the first equation of system (2), we have $x'(t_1) = \lambda > 0$, and hence $x(t) < 0$ for $t \in (t_1 - \epsilon, t_1)$ and sufficiently small $\epsilon > 0$. This contradicts $x(t) > 0$ for $t \in [0, t_1)$. It follows that $x(t) > 0$ for $t > 0$ as long as $x(t)$ exists. From the second equation of (2) we have

$$y(t) = y(0) e^{\int_0^t [\beta x(\theta) - d_2 - \gamma z(\theta)] d\theta}.$$

It follows that $y(t) > 0$ for $t > 0$. Similarly, we can show that $z(t) > 0$ for $t > 0$.

Next we show that positive solutions of (2) are ultimately uniformly bounded for $t \geq 0$. From the first equation of (2), we obtain $x'(t) \leq \lambda - d_1 x(t)$, and thus $\limsup_{t \rightarrow \infty} x(t) \leq \frac{\lambda}{d_1}$. Adding the first two equations of (2) we get

$$\begin{aligned} (x(t) + y(t))' &= \lambda - d_1 x(t) - d_2 y(t) - \gamma y(t)z(t) \\ &\leq \lambda - \tilde{d}(x(t) + y(t)), \end{aligned}$$

where $\tilde{d} = \min\{d_1, d_2\}$. Thus $\limsup_{t \rightarrow \infty} (x(t) + y(t)) \leq \frac{\lambda}{\tilde{d}}$. Adding all the equations of (2) we get

$$\begin{aligned} \left(x(t) + y(t) + \frac{\gamma}{\mu} z(t + \tau)\right)' &= \lambda - d_1 x(t) - d_2 y(t) - d_3 \frac{\gamma}{\mu} z(t + \tau) \\ &\leq \lambda - d \left(x(t) + y(t) + \frac{\gamma}{\mu} z(t + \tau)\right), \end{aligned}$$

where $d = \min\{d_1, d_2, d_3\}$. Thus $\limsup_{t \rightarrow \infty} \left(x(t) + y(t) + \frac{\gamma}{\mu} z(t + \tau)\right) \leq \frac{\lambda}{d}$. Therefore, $x(t)$, $y(t)$ and $z(t)$ are ultimately uniformly bounded in $\mathbb{R} \times \mathcal{C} \times \mathcal{C}$. \square

As a consequence of the proof of Proposition 2.1, we know that the dynamics of system (2) can be analyzed in the following bounded feasible region

$$\Gamma = \left\{ (x, y, v) \in \mathbb{R}_+ \times \mathcal{C}^+ \times \mathcal{C}^+ : |x| \leq \frac{\lambda}{d_1}, \|x + y\| \leq \frac{\lambda}{\tilde{d}}, \left\| x + y + \frac{\gamma}{\mu} z \right\| \leq \frac{\lambda}{d} \right\}.$$

Furthermore, the region Γ is positively invariant with respect to model (2) and the model is well posed.

System (2) always has an infection-free equilibrium $P_0 = (x_0, 0, 0)$, $x_0 = \frac{\lambda}{d_1}$. In addition to P_0 , the system can have two chronic-infection equilibria $P_1 = (\bar{x}, \bar{y}, 0)$ and $P_2 = (x^*, y^*, z^*)$ in Γ , where $\bar{x}, \bar{y}, x^*, y^*, z^*$ are all positive. At equilibrium P_1 , the HTLV-I infection is persistent with a constant proviral load $\bar{y} > 0$, whereas the CTL response is absent, so is the risk for developing HAM/TSP. This corresponds to the situation of an asymptotic carrier. At equilibrium P_2 , both the proviral load and CTL response persists at a constant level. This corresponds to the situation of a HAM/TSP patient. Which of the three steady-states is the final outcome of the system will be determined by a combination of two threshold parameters

$$R_0 = \frac{\lambda\beta}{d_1d_2}, \quad \text{and} \tag{4}$$

$$R_1 = \frac{\lambda\beta\mu}{d_1d_2\mu + \beta d_2d_3}. \tag{5}$$

They are called the basic reproduction numbers for viral infection and for CTL response, respectively (cf. Gomez-Acevedo et al. [10]). We note that $R_1 < R_0$ always holds.

It can be verified that the carrier equilibrium $P_1 = (\bar{x}, \bar{y}, 0)$ exists if and only if $R_0 > 1$, and that

$$\bar{x} = \frac{d_2}{\beta} = \frac{\lambda}{d_1R_0}, \quad \bar{y} = \frac{\lambda\beta - d_1d_2}{\beta d_2} = \frac{d_1(R_0 - 1)}{\beta}. \tag{6}$$

The coordinates of the HAM/TSP equilibrium $P_2 = (x^*, y^*, z^*)$ are given by

$$\begin{aligned} x^* &= \frac{\lambda\mu}{d_1\mu + \beta d_3} = \frac{d_2R_1}{\beta}, & y^* &= \frac{d_3}{\mu}, \\ z^* &= \frac{\beta\lambda\mu - d_1d_2\mu - \beta d_2d_3}{(d_1\mu + \beta d_3)\gamma} = \frac{d_1d_2\mu + \beta d_2d_3}{(d_1\mu + \beta d_3)\gamma} (R_1 - 1). \end{aligned} \tag{7}$$

Therefore, P_2 exists in the interior of Γ if and only if $R_1 > 1$. We thus have the following result.

Proposition 2.2. *If $R_0 \leq 1$, $P_0 = (\frac{\lambda}{d_1}, 0, 0)$ is the only equilibrium in Γ . If $R_1 \leq 1 < R_0$, the carrier equilibrium $P_1 = (\bar{x}, \bar{y}, 0)$ exists and is the only chronic-infection equilibrium in Γ . If $R_1 > 1$, both the carrier equilibrium P_1 and the HAM/TSP equilibrium $P_2 = (x^*, y^*, z^*)$ exist.*

3. Global stability of P_0 when $R_0 \leq 1$

Intuitively, if $R_0 < 1$, the virus will not spread since an infected cell produces on average less than one secondary infection. In this section, we rigorously show that, when $R_0 \leq 1$, the infection-free equilibrium P_0 is globally asymptotically stable in Γ .

Theorem 3.1. *If $R_0 \leq 1$, then the infection-free equilibrium P_0 of system (2) is globally asymptotically stable in Γ . If $R_0 > 1$, then P_0 is unstable.*

Proof. To prove global stability of P_0 , we consider a Lyapunov functional $L : \mathbb{R} \times \mathbb{C} \times \mathbb{C} \rightarrow \mathbb{R}$ given by

$$L(x(t), y_t, z_t) = y_t(0). \tag{8}$$

Here $y_t(s) = y(t + s)$, $z_t(s) = z(t + s)$ for $s \in [-\tau, 0]$, and thus $y(t) = y_t(0)$, $z(t) = z_t(0)$ in this notation. Calculating the time derivative of L along solutions of system (2), we obtain

$$\begin{aligned} L'|_{(2)} &= y'(t) = \beta x(t)y(t) - d_2y(t) - \gamma y(t)z(t) \\ &\leq y(t)(\beta x(t) - d_2) \leq y(t) \left(\beta \frac{\lambda}{d_1} - d_2 \right) = d_2y(t)(R_0 - 1). \end{aligned}$$

Therefore, $R_0 \leq 1$ ensures that $L'|_{(2)} \leq 0$ for all $x(t), y(t), z(t) > 0$, and $L' = 0$ only if $y = 0$ or $R_0 = 1$. It can be verified that the maximal compact invariant set in $\{L'|_{(2)} = 0\}$ is the singleton P_0 . By the LaSalle–Lyapunov theorem [27, Theorem 3.4.7], we conclude that P_0 is globally attractive in Γ if $R_0 \leq 1$. Furthermore, it can be verified that P_0 is locally stable using the same proof as one for Corollary 5.3.1 in [28]. Therefore, P_0 is globally asymptotically stable in Γ when $R_0 \leq 1$.

The characteristic equation of the infection-free equilibrium P_0 is

$$(\xi + d_1) \left(\xi - \frac{\beta\lambda}{d_1} + d_2 \right) (\xi + d_3) = 0. \tag{9}$$

The eigenvalues of (9) are $-d_1$, $\beta\lambda/d_1 - d_2$, and $-d_3$. If $R_0 > 1$, then $\beta\lambda/d_1 - d_2 = d_2(R_0 - 1) > 0$, and P_0 is unstable. □

4. Global stability of P_1 when $R_1 \leq 1 < R_0$

Theorem 4.1. *If $R_1 \leq 1 < R_0$, then the carrier equilibrium P_1 is globally asymptotically stable in $\Gamma \setminus \{x\text{-axis}\}$. If $R_1 > 1$, then P_1 is unstable.*

Proof. Let

$$g(u) = u - \ln u, \quad \text{for } u \in (0, +\infty).$$

Let $P_1 = (\bar{x}, \bar{y}, 0)$ be the carrier equilibrium with \bar{x}, \bar{y} given in (6). Define a Lyapunov functional $V : \mathbb{R} \times \mathcal{C} \times \mathcal{C} \rightarrow \mathbb{R}$

$$V(x(t), y_t, z_t) = \bar{x}g\left(\frac{x(t)}{\bar{x}}\right) + \bar{y}g\left(\frac{y_t(0)}{\bar{y}}\right) + \frac{\gamma}{\mu}z_t(0) + \gamma \int_{-\tau}^0 y_t(\theta)z_t(\theta) d\theta. \tag{10}$$

Since $g : \mathbb{R}_+ \rightarrow \mathbb{R}$ has the global minimum at $u = 1$ and $g(1) = 1$, the Lyapunov functional V is positive definite with respect to P_1 in the interior of Γ . Calculating the time derivative of V along solutions of system (2), we obtain

$$V'|_{(2)} = \lambda - d_1x(t) - \lambda \frac{\bar{x}}{x(t)} + d_1\bar{x} + \beta\bar{x}y(t) - d_2y(t) - \beta\bar{y}x(t) + d_2\bar{y} + \gamma\bar{y}z(t) - \frac{\gamma d_3}{\mu}z(t).$$

Using $\lambda = d_1\bar{x} + \beta\bar{x}\bar{y}$ and $d_2 = \beta\bar{x}$, we obtain

$$\begin{aligned} V'|_{(2)} &= (d_1\bar{x} + \beta\bar{x}\bar{y}) \left(2 - \frac{x(t)}{\bar{x}} - \frac{\bar{x}}{x(t)} \right) + \gamma \left(\bar{y} - \frac{d_3}{\mu} \right) z(t) \\ &= (d_1\bar{x} + \beta\bar{x}\bar{y}) \left(2 - \frac{x(t)}{\bar{x}} - \frac{\bar{x}}{x(t)} \right) + \frac{\gamma(d_1\mu + \beta d_3)}{\beta\mu} (R_1 - 1)z(t) \\ &\leq \frac{\gamma(d_1\mu + \beta d_3)}{\beta\mu} (R_1 - 1)z(t) \leq 0, \quad \text{if } R_1 \leq 1, \end{aligned} \tag{11}$$

since

$$\frac{x(t)}{\bar{x}} + \frac{\bar{x}}{x(t)} - 2 \geq 0.$$

Furthermore, $V' = 0$ implies that $x(t) = \bar{x}$ and $z(t) = 0$, and thus the maximal compact invariant set in the set where $V' = 0$ is the singleton $\{P_1\}$. Positive definiteness of V with respect to P_1 and a similar argument as in the proof of Theorem 3.1 prove that, when $R_1 \leq 1 < R_0$, P_1 is globally asymptotically stable in $\Gamma \setminus \{x\text{-axis}\}$. Along the invariant x -axis, solutions converge to the infection-free equilibrium P_0 .

When $R_1 > 1$ and for $x(t) > 0$ such that $|x(0) - x_0|$ is sufficiently small, we have $V'|_{(2)} > 0$ from (11). Therefore, the carrier equilibrium P_1 is locally unstable by the standard Lyapunov instability theorem [29]. \square

Proposition 2.1, Theorems 3.1 and 4.1 completely characterize the global dynamics of system (2) for the cases when $R_1 \leq 1$. They establish R_0 and R_1 as two sharp threshold parameters that together determine the outcomes of the HTLV-I infection:

- (i) If $R_0 \leq 1$, then the HTLV-I viruses are cleared.
- (ii) If $R_1 \leq 1 < R_0$, then HTLV-I infection becomes chronic with no persistent CTL response. The patient remains as an asymptotic carrier.
- (iii) If $R_1 > 1$, then both HTLV-I infection and CTL response will persist. The patient has a high risk of developing HAM/TSP.

We note that the existence of the carrier equilibrium P_1 has been neglected in many earlier modeling studies of HTLV-I infection and its CTL response. Since HTLV-I infection is lifelong [6], the virus is rarely cleared from the body. Accordingly, the infection-free equilibrium P_0 is not expected to be achieved for a person infected with HTLV-I. The dynamical outcomes that are biologically relevant are the carrier state P_1 and HAM/TSP state P_2 . Furthermore, considering the majority of HTLV-I infected population are asymptomatic carriers, a realistic control and treatment strategy for HAM/TSP is to prevent carriers from developing HAM/TSP by keeping the threshold parameter R_1 below 1, rather than reducing R_0 to below 1, a more difficult task given that $R_1 < R_0$.

5. Dynamics when $R_1 > 1$

We have shown in Theorem 4.1 that, if $R_1 > 1$, both the infection-free equilibrium P_0 and the carrier equilibrium P_1 are unstable, and the HAM/TSP equilibrium P_2 exists in the interior of Γ . The patient has a high risk of developing HAM/TSP. In this section, we investigate the temporal dynamics of the interaction of HTLV-I infection and the HTLV-I specific CTL response. Earlier numerical evidence has shown that P_2 can lose its stability and sustained oscillations can exist. We will investigate the stability of P_2 and identify parameter regions in which the time delay can destabilize P_2 and lead to Hopf bifurcation.

5.1. Stability of P_2 and local Hopf bifurcation

We first translate P_2 to the origin through a change of variables $x_1(t) = x(t) - x^*$, $y_1(t) = y(t) - y^*$, $z_1(t) = z(t) - z^*$. Then system (2) becomes

$$\begin{aligned} x_1'(t) &= -(\beta y^* + d_1)x_1(t) - \beta x^* y_1(t) - \beta x_1(t)y_1(t), \\ y_1'(t) &= \beta y^* x_1(t) - \gamma y^* z_1(t) + \beta x_1(t)y_1(t) - \gamma y_1(t)z_1(t), \\ z_1'(t) &= \mu z^* y_1(t - \tau) + d_3 z_1(t - \tau) - d_3 z_1(t) + \mu y_1(t - \tau)z_1(t - \tau). \end{aligned} \tag{12}$$

The characteristic equation associated with the linearization of system (12) at $(0, 0, 0)$ is

$$\xi^3 + a_2 \xi^2 + a_1 \xi + a_0 + (b_2 \xi^2 + b_1 \xi + b_0) e^{-\xi \tau} = 0, \tag{13}$$

where

$$\begin{aligned} a_2 &= d_3 + \beta y^* + d_1, & a_1 &= d_3(\beta y^* + d_1) + \beta^2 x^* y^*, & a_0 &= \beta^2 x^* y^* d_3, \\ b_2 &= -d_3, & b_1 &= \gamma d_3 z^* - d_3(\beta y^* + d_1), & b_0 &= \gamma d_3 z^*(\beta y^* + d_1) - \beta^2 x^* y^* d_3. \end{aligned}$$

When $\tau = 0$, Eq. (13) becomes

$$\xi^3 + (a_2 + b_2)\xi^2 + (a_1 + b_1)\xi + (a_0 + b_0) = 0.$$

Noticing that

$$\begin{aligned} a_2 + b_2 &= \beta y^* + d_1 > 0, & a_1 + b_1 &= \gamma d_3 z^* + \beta^2 x^* y^* > 0, \\ a_0 + b_0 &= \gamma d_3 z^*(\beta y^* + d_1) > 0, \\ (a_2 + b_2)(a_1 + b_1) - (a_0 + b_0) &= \beta^2 x^* y^*(\beta y^* + d_1) > 0, \end{aligned}$$

and by the Routh–Hurwitz criterion, we know that all roots of Eq. (13) when $\tau = 0$ have negative real parts. We obtain the following result.

Proposition 5.1. *Suppose $R_1 > 1$. Then the HAM/TSP equilibrium P_2 of system (2) is locally asymptotically stable when $\tau = 0$.*

Remark. Using a Lyapunov function

$$U(x, y, z) = (x - x^* \ln x) + (y - y^* \ln y) + \frac{\gamma}{\mu}(z - z^* \ln z),$$

we can show that, if $R_1 > 1$ and when $\tau = 0$, equilibrium P_2 of system (2) is globally asymptotically stable in the interior of Γ .

Time delays are known to cause destabilization of equilibria and produce oscillations through Hopf bifurcations. We will use the delay $\tau > 0$ as a bifurcation parameter and investigate stability changes at the HAM/TSP equilibrium P_2 . We will show that Hopf bifurcation occurs for an open set of parameter values. This rigorously establishes that periodic oscillations exist in model (2). Since, when $\tau = 0$, all roots of the characteristic Eq. (13) lie to the left of the imaginary axis, a stability change at P_2 can only happen when characteristic roots cross the imaginary axis to the right. We thus consider the possibility of purely imaginary roots $\xi = i\omega$ ($\omega > 0$) for $\tau > 0$. Substituting $\xi = i\omega$ into Eq. (13) and separating the real and imaginary parts, we obtain

$$\begin{aligned} -\omega^3 + a_1 \omega &= (b_0 - b_2 \omega^2) \sin \omega \tau - b_1 \omega \cos \omega \tau, \\ a_2 \omega^2 - a_0 &= (b_0 - b_2 \omega^2) \cos \omega \tau + b_1 \omega \sin \omega \tau. \end{aligned} \tag{14}$$

Squaring and adding both equations of (14) lead to

$$F(\omega) = \omega^6 + (a_2^2 - b_2^2 - 2a_1)\omega^4 + (a_1^2 - 2a_0a_1 - b_1^2 + 2b_0b_2)\omega^2 + (a_0^2 - b_0^2) = 0. \tag{15}$$

Let

$$G(u) = u^3 + (a_2^2 - b_2^2 - 2a_1)u^2 + (a_1^2 - 2a_0a_1 - b_1^2 + 2b_0b_2)u + (a_0^2 - b_0^2). \tag{16}$$

Therefore, if $i\omega$ ($\omega > 0$) is a purely imaginary root of Eq. (13), then we have the equation

$$G(u) = 0 \tag{17}$$

has a positive root $u = \omega^2$. Note that

$$G'(u) = 3u^2 + 2(a_2^2 - b_2^2 - 2a_1)u + a_1^2 - 2a_0a_1 - b_1^2 + 2b_0b_2.$$

Let

$$\Delta = (a_2^2 - b_2^2 - 2a_1)^2 - 3(a_1^2 - 2a_0a_1 - b_1^2 + 2b_0b_2). \tag{18}$$

Then

(1) If $\Delta \leq 0$, then $G'(u) \geq 0$, and thus $G(u)$ is monotonically increasing. Therefore, when $a_0^2 - b_0^2 = G(0) \geq 0$ and $\Delta \leq 0$, Eq. (17) has no positive roots, and all characteristic roots will remain to the left of the imaginary axis for all $\tau > 0$.

- (2) If $a_0^2 - b_0^2 < 0$, since $\lim_{u \rightarrow \infty} G(u) = \infty$, we know that (17) has at least one positive root, and characteristic roots can cross the imaginary axis.
- (3) If $\Delta > 0$, then the graph of $G(u)$ has critical points

$$u^* = \frac{-(a_2^2 - b_2^2 - 2a_1) + \sqrt{\Delta}}{3}, \quad u^{**} = \frac{-(a_2^2 - b_2^2 - 2a_1) - \sqrt{\Delta}}{3}. \tag{19}$$

If $u^* > 0$ and $G(u^*) < 0$, then $G(u) = 0$ has positive roots.

Let $u_i, 1 \leq i \leq 3$, be the positive roots of $G(u) = 0$ and $\omega_i = \sqrt{u_i}$. Solving Eq. (14) for τ yields

$$\tau_i = \frac{1}{\omega_i} \arccos \left\{ \frac{(b_1 - a_2 b_2) \omega_i^4 + (a_0 b_2 + a_2 b_0 - a_1 b_1) \omega_i^2 - a_0 b_0}{(b_2 \omega_i^2 - b_0)^2 + b_1^2 \omega_i^2} \right\}, \quad 1 \leq i \leq 3. \tag{20}$$

Define

$$\tau_0 = \tau_k = \min_{1 \leq i \leq 3} \{ \tau_i \mid u_i \text{ is a positive solution of } G(u) = 0 \}, \tag{21}$$

$$\omega_0 = \omega_k.$$

Then τ_0 is the first value of τ when a pair characteristic roots cross the imaginary axis at $\pm i\omega_0$. We thus obtain the following result.

Theorem 5.2. (1) If $a_0 - b_0 \geq 0$ and $\Delta \leq 0$, then the HAM/TSP equilibrium P_2 remains asymptotically stable for all $\tau \geq 0$.
 (2) If either (a) $a_0 - b_0 < 0$,

$$\text{or (b) } \Delta > 0, u^* = \frac{-(a_2^2 - b_2^2 - 2a_1) + \sqrt{\Delta}}{3} > 0 \text{ and } G(u^*) < 0,$$

then there exist $\tau_0 > 0$ and ω_0 as in (21), such that the HAM/TSP equilibrium P_2 is asymptotically stable for $\tau \in [0, \tau_0)$. Furthermore, if $G'(\omega_0^2) \neq 0$, then system (2) undergoes a Hopf bifurcation at the HAM/TSP equilibrium P_2 when $\tau = \tau_0$.

Proof. It remains to show the transversality condition for the Hopf bifurcation holds at $\tau = \tau_0$. Differentiating Eq. (13) with respect to τ we obtain

$$\left[\frac{d\xi}{d\tau} \right]^{-1} = \frac{(3\xi^2 + 2a_2\xi + a_1) e^{\xi\tau}}{\xi(b_2\xi^2 + b_1\xi + b_0)} + \frac{2b_2\xi + b_1}{\xi(b_2\xi^2 + b_1\xi + b_0)} - \frac{\tau}{\xi}.$$

Using (14) we obtain

$$\begin{aligned} \left[\frac{d(\text{Re}\xi(\tau))}{d\tau} \right]_{\tau=\tau_0}^{-1} &= \text{Re} \left[\frac{(3\xi^2 + 2a_2\xi + a_1) e^{\xi\tau}}{\xi(b_2\xi^2 + b_1\xi + b_0)} \right]_{\tau=\tau_0} + \text{Re} \left[\frac{2b_2\xi + b_1}{\xi(b_2\xi^2 + b_1\xi + b_0)} \right]_{\tau=\tau_0} \\ &= \frac{1}{b_1^2\omega_0^2 + (b_0 - b_2\omega_0^2)^2} \{ (a_1 - 3\omega_0^2)\omega_0[(b_0 - b_2\omega_0^2) \sin \omega_0\tau_0 - b_1\omega_0 \cos \omega_0\tau_0] \\ &\quad + 2a_2\omega_0^2[(b_0 - b_2\omega_0^2) \cos \omega_0\tau_0 + b_1\omega_0 \sin \omega_0\tau_0] - b_1^2\omega_0^2 + 2b_2\omega_0^2(b_0 - b_2\omega_0^2) \} \\ &= \frac{3\omega_0^6 + 2(a_2^2 - b_2^2 - 2a_1)\omega_0^4 + (a_1^2 - 2a_0a_1 - b_1^2 + 2b_0b_2)\omega_0^2}{b_1^2\omega_0^4 + \omega_0^2(b_0 - b_2\omega_0^2)^2} \\ &= \frac{G'(\omega_0^2)}{b_1^2\omega_0^2 + (b_0 - b_2\omega_0^2)^2}. \end{aligned}$$

Therefore

$$\text{sign} \left[\frac{d(\text{Re}\xi(\tau))}{d\tau} \right]_{\tau=\tau_0} = \text{sign} G'(\omega_0^2).$$

Therefore, if $G'(\omega_0^2) \neq 0$, the transversality condition holds and a Hopf bifurcation occurs at $\tau = \tau_0$. This completes the proof. □

In fact, we can obtain more information on the transversality condition. If $G'(\omega_0^2) \neq 0$, then $\frac{d(\text{Re}\xi(\tau_0))}{d\tau} \neq 0$. If $\frac{d(\text{Re}\xi(\tau_0))}{d\tau} < 0$, then characteristic Eq. (13) has roots with positive real parts for $\tau < \tau_0$ and close to τ_0 . This contradicts that fact P_2 is asymptotically stable for $0 \leq \tau < \tau_0$ as in Theorem 5.2(2). Thus, we obtain the following proposition.

Proposition 5.3. Suppose $G'(\omega_0^2) \neq 0$. Then $\frac{d(\text{Re}\xi(\tau_0))}{d\tau} > 0$.

In Theorem 5.2, we have identified parameter regimes in which delay τ can destabilize the HAM/TSP equilibrium and lead to a Hopf bifurcation. This shows that, when $\tau > \tau_0$ and is close to τ_0 , periodic solutions exist. As a consequence, when HAM/TSP develops, the CD4⁺ count, proviral load, and the HTLV-I-specific CTL frequency can oscillate around the equilibrium level. In the next section, we will demonstrate that these periodic solutions tend to be stable.

5.2. Stability of the bifurcating periodic solutions

In this subsection, we investigate the stability of the bifurcating periodic solutions, using a procedure in Hassard et al. [30].

Let $\tau = \tau_0 + \mu$, and we use μ as the bifurcation parameter with $\mu = 0$ the Hopf bifurcation value. We first scale the time $t \mapsto (t/\tau)$ in system (12) and set

$$B_1 = \begin{pmatrix} -(\beta y^* + d_1) & -\beta x^* & 0 \\ \beta y^* & 0 & -\gamma y^* \\ 0 & 0 & -d_3 \end{pmatrix}, \quad B_2 = \begin{pmatrix} 0 & 0 & 0 \\ 0 & 0 & 0 \\ 0 & \mu z^* & d_3 \end{pmatrix}.$$

Define an operator $L_\mu : \mathbb{C}([-1, 0], \mathbb{R}^3) \rightarrow \mathbb{R}^3$ as

$$L_\mu(\phi) = (\tau_0 + \mu)B_1\phi(0) + (\tau_0 + \mu)B_2\phi(-1),$$

with

$$f(\mu, \phi) = (\tau_0 + \mu) \begin{pmatrix} -\beta\phi_1(0)\phi_2(0) \\ \beta\phi_1(0)\phi_2(0) - \gamma\phi_2(0)\phi_3(0) \\ \mu\phi_2(-1)\phi_3(-1) \end{pmatrix},$$

for $\phi = (\phi_1, \phi_2, \phi_3)^T \in \mathbb{C}([-1, 0], \mathbb{R}^3)$. We can rewrite system (12) as an abstract FDE in $\mathbb{C}([-1, 0], \mathbb{R}^3)$

$$\dot{v}(t) = L_\mu(v_t) + f(\mu, v_t), \tag{22}$$

where $v(t) = (x_1(t), y_1(t), z_1(t))^T \in \mathbb{R}^3$. Let

$$\delta(\theta) = \begin{cases} 0, & \theta \neq 0, \\ 1, & \theta = 0, \end{cases}$$

and define

$$\eta(\theta, \mu) = (\tau_0 + \mu)B_1\delta(\theta) - (\tau_0 + \mu)B_2\delta(\theta + 1).$$

Then operator L_μ in (22) can be represented in an integral form as

$$L_\mu\phi = \int_{-1}^0 d\eta(\theta, 0)\phi(\theta), \quad \text{for } \phi \in \mathbb{C}([-1, 0], \mathbb{R}^3).$$

Define operators

$$A(\mu)\phi(\theta) = \begin{cases} \frac{d\phi(\theta)}{d\theta}, & \theta \in [-1, 0), \\ \int_{-1}^0 d\eta(s, \mu)\phi(s), & \theta = 0 \end{cases}$$

and

$$R(\mu)\phi(\theta) = \begin{cases} 0, & \theta \in [-1, 0), \\ f(\mu, \phi), & \theta = 0. \end{cases}$$

Then system (22) is written as an abstract ordinary differential equation in the Banach space $\mathbb{C}([-1, 0], \mathbb{R}^3)$

$$\dot{v}_t = A(\mu)v_t + R(\mu)v_t.$$

For $\psi \in \mathbb{C}^1([0, 1], (\mathbb{R}^3)^*)$, define an operator

$$A^*\psi(s) = \begin{cases} -\frac{d\psi(s)}{ds}, & s \in (0, 1], \\ \int_{-1}^0 d\eta^T(t, 0)\phi(-t), & s = 0 \end{cases}$$

and a bilinear form

$$\langle \psi(s), \phi(\theta) \rangle = \bar{\psi}(0)\phi(0) - \int_{-1}^0 \int_{\xi=0}^\theta \bar{\psi}(\xi - \theta) d\eta(\theta)\phi(\xi) d\xi,$$

where $\eta(\theta) = \eta(\theta, 0)$. Then $A(0)$ and A^* are adjoint operators with respect to this bilinear form. From the previous section, we know that $\pm i\omega_0\tau_0$ are eigenvalues of $A(0)$ and therefore they are also eigenvalues of A^* .

Let

$$\begin{aligned} (1, q_2, q_3)^T &= \left(1, -\frac{i\omega_0 + d_1 + \beta y^*}{\beta x^*}, \frac{\beta}{\gamma} + \frac{i\omega_0(i\omega_0 + d_1 + \beta y^*)}{\beta \gamma x^* y^*} \right)^T, \\ (1, q_2^*, q_3^*) &= \left(1, \frac{-i\omega_0 + d_1}{\beta y^*} + 1, \frac{\beta^2 x^* y^* - \omega_0^2 - i\omega_0(d_1 + \beta y^*)}{\beta d_3 z^* e^{i\omega_0 \tau_0}} \right), \\ D &= (1 + \bar{q}_2 q_2^* + \bar{q}_3 q_3^* + (\mu z^* \bar{q}_2 q_3^* + d_3 \bar{q}_3 q_3^*) \tau_0 e^{i\omega_0 \tau_0})^{-1}. \end{aligned}$$

It can be verified that the vectors $q(\theta) = (1, q_2, q_3)^T e^{i\theta \omega_0 \tau_0}$, $\theta \in [-1, 0]$, and $q^*(s) = D(1, q_2^*, q_3^*) e^{is\omega_0 \tau_0}$, $s \in [0, 1]$, are the eigenvectors of $A(0)$ and A^* corresponding to the eigenvalue $i\omega_0 \tau_0$ and $-i\omega_0 \tau_0$, respectively. Furthermore $\langle q^*(s), q(\theta) \rangle = 1$, $\langle q^*(s), \bar{q}(\theta) \rangle = 0$.

Following the procedure in [30], we obtain the coefficients:

$$\begin{aligned} g_{20} &= 2\tau_0 \bar{D} \left[-q_2^2 + \bar{q}_2^* q_2^2 - \bar{q}_2^* q_2 q_3^2 + \mu \bar{q}_3^* q_3 q_2 e^{-2i\omega_0 \tau_0} \right], \\ g_{11} &= 2\tau_0 \bar{D} \left[(-q_2 + \bar{q}_2^* q_2) \text{Re} q_2 + (-\bar{q}_2^* q_3 + \mu \bar{q}_3^*) \text{Re}(q_2 \bar{q}_3) \right], \\ g_{02} &= 2\tau_0 \bar{D} \left[(-1 + \bar{q}_2^*) |q_2|^2 - \bar{q}_2^* \bar{q}_2 |q_3|^2 + \mu \bar{q}_3^* \bar{q}_3 q_2 e^{2i\omega_0 \tau_0} \right], \\ g_{21} &= 2\tau_0 \bar{D} \left[(-q_2 + \bar{q}_2^* q_2) \left[\frac{W_{20}^{(1)}(0)}{2} \bar{q}_2 + W_{11}^{(1)}(0) q_2 + \frac{W_{20}^{(2)}(0)}{2} + W_{11}^{(2)}(0) \right] \right. \\ &\quad \left. - \bar{q}_2^* q_3 \left[\frac{W_{20}^{(3)}(0)}{2} \bar{q}_2 + W_{11}^{(3)}(0) q_2 + \frac{W_{20}^{(2)}(0)}{2} \bar{q}_3 + W_{11}^{(2)}(0) q_3 \right] \right. \\ &\quad \left. + \mu \bar{q}_3^* \left[\frac{W_{20}^{(2)}(-1)}{2} \bar{q}_3 e^{i\omega_0 \tau_0} + W_{11}^{(2)}(-1) q_3 e^{-i\omega_0 \tau_0} + \frac{W_{20}^{(3)}(-1)}{2} \bar{q}_2 e^{i\omega_0 \tau_0} + W_{11}^{(3)}(-1) q_2 e^{-i\omega_0 \tau_0} \right] \right], \end{aligned}$$

where for $\theta \in [-1, 0]$,

$$\begin{aligned} W_{20}(\theta) &= \frac{i g_{20}}{\omega_0 \tau_0} q(\theta) + \frac{i \bar{g}_{02}}{3\omega_0 \tau_0} \bar{q}(\theta) + E_1 e^{2i\theta \omega_0 \tau_0}, \\ W_{11}(\theta) &= -\frac{i g_{11}}{\omega_0 \tau_0} q(\theta) + \frac{i \bar{g}_{11}}{\omega_0 \tau_0} \bar{q}(\theta) + E_2, \\ E_1 &= 2G^{-1} \begin{pmatrix} -q_2^2 \\ q_2^2 - q_2 q_3^2 \\ \mu q_2 q_3 e^{-2i\omega_0 \tau_0} \end{pmatrix}, \end{aligned}$$

where

$$G = \begin{pmatrix} 2i\omega_0 + \beta y^* + d_1 & \beta x^* & 0 \\ -\beta y^* & 2i\omega_0 & \gamma y^* \\ 0 & -\mu z^* e^{-2i\omega_0 \tau_0} & 2i\omega_0 + d_3 - d_3 e^{-2i\omega_0 \tau_0} \end{pmatrix},$$

and

$$E_2 = 2 \begin{pmatrix} \beta y^* + d_1 & \beta x^* & 0 \\ -\beta y^* & 0 & \gamma y^* \\ 0 & -\mu z^* & 0 \end{pmatrix}^{-1} \begin{pmatrix} -q_2 \text{Re} q_2 \\ q_2 \text{Re} q_2 - q_3 \text{Re}(q_2 \bar{q}_3) \\ \mu \text{Re}(q_2 \bar{q}_3) \end{pmatrix}.$$

Consequently, g_{21} can be expressed explicitly, and we can compute the following quantities:

$$\begin{aligned} c_1(0) &= \frac{i}{2\omega_0 \tau_0} \left(g_{11} g_{20} - 2|g_{11}|^2 - \frac{|g_{02}|^2}{3} \right) + \frac{g_{21}}{2}, \\ \mu_2 &= -\frac{\text{Re}(c_1(0))}{\text{Re}(\xi'(\tau_0))}, \\ \beta_2 &= 2\text{Re}(c_1(0)). \end{aligned} \tag{23}$$

The sign of μ_2 determines the direction of the Hopf bifurcation: if $\mu_2 > 0$ ($\mu_2 < 0$), then the bifurcating periodic solutions exists for $\tau > \tau_0$ ($\tau < \tau_0$); and the sign of β_2 determines the stability of bifurcating periodic solutions: they are stable (unstable) if $\beta_2 < 0$ ($\beta_2 > 0$). From Proposition 5.3, $\text{Re}(\xi'(\tau_0)) > 0$, and thus $\text{sign} \mu_2 = -\text{sign} \text{Re} c_1(0)$. The following result holds.

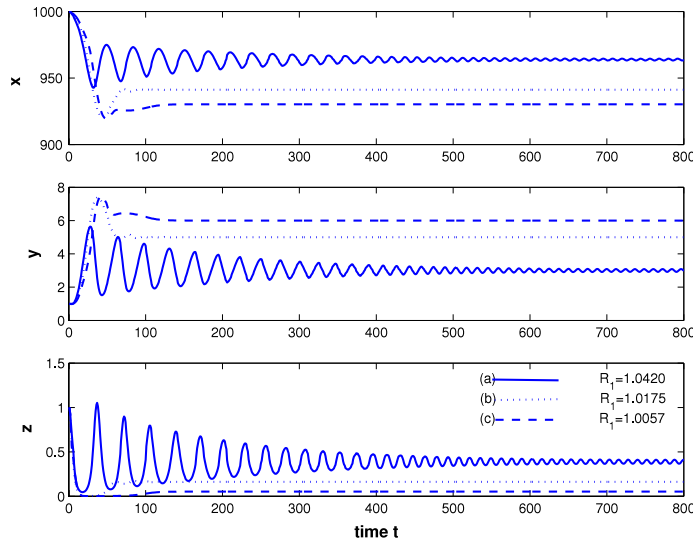


Fig. 2. When conditions of Theorem 5.2(1) hold, the HAM/TSP equilibrium P_2 of system (2) is local asymptotically stable for all $\tau \geq 0$. Here $\lambda = 160$, $\beta = 0.002$, $d_1 = 0.16$, $d_2 = 1.85$, $\gamma = 0.2$, $\mu = 0.2$, and $d_3 = 0.6$ in (a), $d_3 = 1$ in (b), $d_3 = 1.2$ in (c).

Theorem 5.4. Assume that conditions of Theorem 5.2(2) hold. Then

- (1) if $\text{Re}(c_1(0)) < 0$, then there exist periodic solutions bifurcating from P_2 for $\tau > \tau_0$, and they are orbitally asymptotically stable as $t \rightarrow \infty$;
- (2) if $\text{Re}(c_1(0)) > 0$, then the bifurcating periodic solutions exist for $\tau < \tau_0$, and they are orbitally asymptotically stable as $t \rightarrow -\infty$.

Though the complexity in the expression of $\text{Re}(c_1(0))$ will not allow direct verification of its sign for arbitrary parameter values, formula derived in (23) are useful for verifying stability of bifurcating periodic solutions for a specific set of parameter values.

6. Numerical simulations

In this section, we carry out numerical simulations to illustrate and support our analytical results on the change of stability of P_2 and the occurrence of Hopf bifurcation for several values of the time delay.

For case (1) of Theorem 5.2, under conditions $a_0 - b_0 \geq 0$ and $\Delta \leq 0$, the HAM/TSP equilibrium P_2 is locally asymptotically stable irrespective of the time delay τ . Our numerical simulations show that the time delay can cause damped oscillations in all compartments, see Fig. 2. Biologically, this implies that time delays in CTL response can cause transient fluctuations in the proviral load and the CTL frequency in the early stage of infection, while in a longer term these quantities will stabilize at a constant level.

Figs. 3–5 describe the phenomenon stated in case (2) of Theorem 5.2. We have chosen a set of parameters as follows:

$$\lambda = 160, \quad \beta = 0.002, \quad d_1 = 0.16, \quad d_2 = 1.85, \quad \gamma = 0.2, \quad \mu = 0.2, \quad d_3 = 0.4. \quad (24)$$

Correspondingly, $R_1 = 1.0547 > 1$ and $P_2 = (975.6098, 2, 0.5061)$. It can be verified that the conditions of Theorem 5.2(2) are satisfied. We can compute that $\omega_0 = 0.1881$ and $\tau_0 \doteq 0.7458$. By Theorem 5.2, the HAM/TSP equilibrium P_2 is locally asymptotically stable when $\tau < \tau_0$ (Fig. 3), and Hopf bifurcation occurs at $\tau = \tau_0$; a periodic solution exists when $\tau > \tau_0$ (Fig. 4). Furthermore, we compute $c_1(0) = -0.0233 + 0.0054i$. Therefore $\text{Re}(c_1(0)) < 0$. By Theorem 5.4, we know that the Hopf bifurcation is supercritical: the bifurcating periodic solutions exist for $\tau > \tau_0$ and they are orbitally asymptotically stable. Numerical simulations shown in Figs. 4 and 5 support our analytical results. In Fig. 5(a), we show a global Hopf branch of periodic solutions emanating from the Hopf bifurcation point. In Fig. 5(b), we show that the Floquet multipliers associated with the bifurcating periodic solutions all lie inside the unit circle. All of our numerical simulations are carried out using DDE32 package in Matlab. Bifurcation diagrams in Fig. 5 are produced using DDE-BIFTOOL developed by Engelborghs et al. [31,32].

7. Summary and discussions

We have considered a mathematical model for the cytotoxic T-cell (CTL) response to the infection of CD4⁺ T cells *in vivo* by human T cell leukemia virus type I (HTLV-I). The model incorporates a time lag in the antigenic activation process of CTLs.

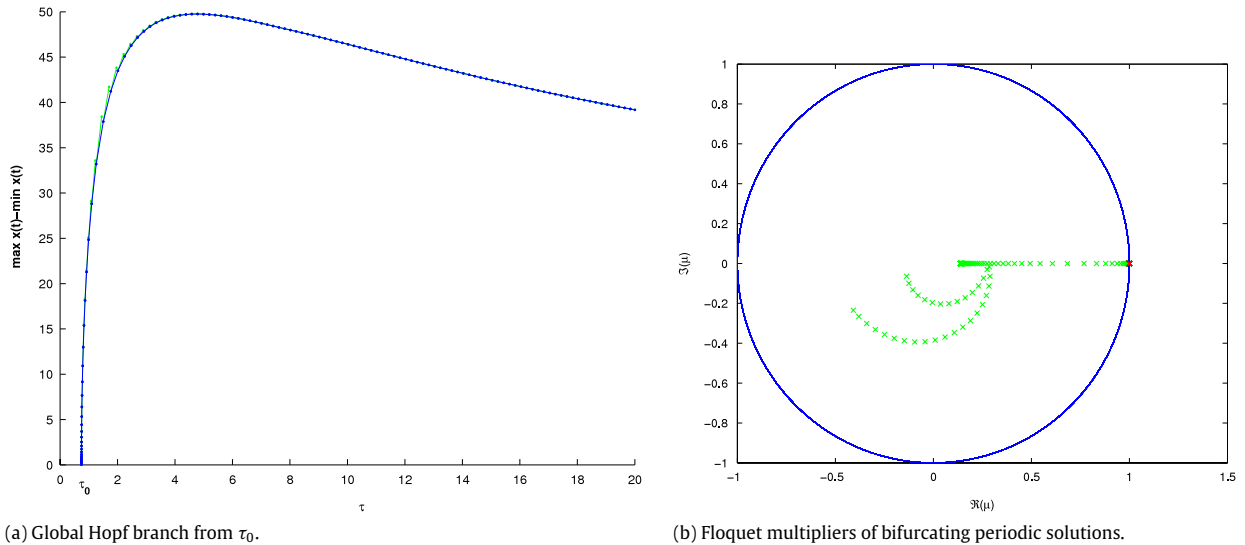


Fig. 5. Numerical exploration of global Hopf bifurcations.

When $R_1 > 1$, we show that the HAM/TSP equilibrium P_2 is asymptotically stable when the delay τ is small, and that increases in the delay τ can destabilize P_2 and lead to Hopf bifurcation and stable periodic solutions. This suggests that as HAM/TSP develops, the proviral load and CTL frequency can either stabilize at a constant level or show oscillations. Stable periodic oscillations have been observed in other models of CTL response to HTLV-I infection *in vivo*. Mechanisms leading to stable oscillations include mitosis division in the HTLV-I-infected CD4⁺ T-cell population [16] or general CTL response functions [34]. Our results, together with numerical studies in [24], establish that time delays in the CTL activation process can also lead to stable oscillations.

Acknowledgments

The research was supported in part by grants from the Natural Science and Engineering Research Council (NSERC), Canada Foundation for Innovation (CFI), National Natural Science Foundation of China (NNSF, No. 10771045) and Program of Excellent Team at HIT. H. Shu acknowledges the financial support of a scholarship from the China Scholarship Council while visiting the University of Alberta. Both authors acknowledge the support from the Mathematics of Information Technology and Complex Systems (MITACS).

References

- [1] F.W. Robbins, A mathematical model of HIV infection: simulating T4, T8, macrophages, antibody, and virus via specific anti-HIV response in the presence of adaptation and tropism, *Bull. Math. Biol.* 72 (2010) 1208–1253.
- [2] K. Wang, A. Fan, et al., Global properties of an improved hepatitis B virus model, *Nonlinear Anal. RWA* 11 (2010) 3131–3138.
- [3] A.M. Elaiw, Global properties of a class of HIV models, *Nonlinear Anal. RWA* 11 (2010) 2253–2263.
- [4] I.T. Vieira, R.C.H. Cheng, et al., Small world network models of the dynamics of HIV infection, *Ann. Oper. Res.* 178 (2010) 173–200.
- [5] Y. Yu, J.J. Nieto, et al., A viral infection model with a nonlinear infection rate, *Bound. Value Probl.* 2009 (2009) Article ID 958016, 19 pages.
- [6] C.R.M. Bangham, The immune response to HTLV-I, *Curr. Opin. Immunol.* 12 (2000) 397–402.
- [7] C.R.M. Bangham, The immune control and cell-to-cell spread of human T-lymphotropic virus type 1, *J. Gen. Virol.* 84 (2003) 3177–3189.
- [8] S. Jacobson, Immunopathogenesis of human T cell lymphotropic virus type I-associated neurologic disease, *J. Infect. Dis.* 186 (S2) (2002) S187–S192.
- [9] N. Eshima, M. Tabata, et al., Population dynamics of HTLV-I infection: a discrete-time mathematical epidemic model approach, *Math. Med. Biol.* 20 (2003) 29–45.
- [10] H. Gomez-Acevedo, M.Y. Li, S. Jacobson, Multi-stability in a model for CTL response to HTLV-I infection and its consequences in HAM/TSP development and prevention, *Bull. Math. Biol.* 72 (2010) 681–696.
- [11] O. Gout, M. Baulac, et al., Medical intelligence: rapid development of myelopathy after HTVL-I Infections acquired by transfusion during cardiac transplantation, *N. Engl. J. Med.* 322 (1990) 383–388.
- [12] M. Osame, R. Janssen, et al., Nationwide survey of HTLV-I-associated myelopathy in Japan: association with blood transfusion, *Ann. Neurol.* 28 (1990) 50–56.
- [13] R. Kubota, M. Osame, S. Jacobson, Retrovirus: human T-cell lymphotropic virus type I-associated diseases and immune dysfunction, in: M.W. Cunningham, R.S. Fujinami (Eds.), *Effects of Microbes on the Immune System*, Lippincott Williams & Wilkins, 2000, pp. 349–371.
- [14] R.C. Gallo, History of the discoveries of the first human retroviruses: HTLV-1 and HTLV-2, *Oncogene* 24 (2005) 5926–5930.
- [15] J.M. Coffin, S.H. Hughes, H.E. Varmus, *Retroviruses*, Cold Spring Harbor Laboratory Press, New York, 1997.
- [16] D. Wodarz, M.A. Nowak, C.R.M. Bangham, The dynamics of HTLV-I and the CTL response, *Immunol. Today* 20 (1999) 220–227.
- [17] M.A. Nowak, R.M. May, *Virus Dynamics: Mathematical Principles of Immunology and Virology*, Oxford University Press, 2000.
- [18] D. Wodarz, C.R.M. Bangham, Evolutionary dynamics of HTLV-I, *J. Mol. Evol.* 50 (2000) 448–455.
- [19] A.S. Perelson, P.W. Nelson, Mathematical analysis of HIV-I dynamics *in vivo*, *SIAM Rev.* 41 (1999) 3–44.
- [20] R.J. De Boer, A.S. Perelson, Towards a general function describing T cell proliferation, *J. Theoret. Biol.* 175 (1995) 567–576.
- [21] R.J. De Boer, A.S. Perelson, Target cell limited and immune control models of HIV infection: a comparison, *J. Theoret. Biol.* 190 (1998) 201–214.

- [22] M.A. Nowak, C.R.M. Bangham, Population dynamics of immune responses to persistent viruses, *Science* 272 (1996) 74–79.
- [23] N. Burić, M. Mudrinic, N. Vasović, Time delay in a basic model of the immune response, *Chaos Solitons Fractals* 12 (2001) 483–489.
- [24] K. Wang, W. Wang, et al., Complex dynamic behavior in a viral model with delayed immune response, *Physica D* 226 (2007) 197–208.
- [25] M.Y. Li, H. Shu, Impact of intracellular delays and target-cell dynamics on *in vivo* viral infections, *SIAM J. Appl. Math.* 70 (2010) 2434–2448.
- [26] C.C. McCluskey, Global stability for an SEIR epidemiological model with varying infectivity and infinite delay, *Math. Biosci. Eng.* 6 (2009) 603–610.
- [27] J. LaSalle, S. Lefschetz, *Stability by Lyapunov's Direct Method*, Academic Press, New York, 1961.
- [28] J.K. Hale, S.V. Lunel, *Introduction to Functional Differential Equations*, Springer-Verlag, New York, 1993.
- [29] J.K. Hale, *Theory of Functional Differential Equations*, Springer-Verlag, Berlin, 1977.
- [30] B.D. Hassard, N.D. Kazarinoff, Y.H. Wan, *Theory and Applications of Hopf Bifurcation*, Cambridge University Press, Cambridge, 1981.
- [31] K. Engelborghs, T. Luzyanina, D. Roose, Numerical bifurcation analysis of delay differential equations using DDE-BIFTOOL, *ACM Trans. Math. Software* 28 (2002) 1–21.
- [32] K. Engelborghs, T. Luzyanina, G. Samaey, DDE-BIFTOOL v. 2.00: A Matlab package for bifurcation analysis of delay differential equations, Technical Report TW-330, Department of Computer Science, K. U. Leuven, Leuven, Belgium, 2001.
- [33] H. Kato, Y. Koya, et al., Oral administration of human T-cell leukemia virus type 1 induces immune unresponsiveness with persistent infection in adult rats, *J. Virol.* 72 (1998) 7289–7293.
- [34] J. Lang, M.Y. Li, Stable and transient periodic oscillations in a mathematical model for CTL response to HTLV-I infection, *J. Math. Biol.* (2011) doi:10.1007/s00285-011-0455-z.